REPORT DOCUMENTATION PAGE

Form Approved OMB NO. 0704-0188

1. REPORT DATE (DD-MM-YYYY)	2. REPORT TYPE	3. DATES COVERED (From - To)
22-08-2012	Final Report	17-Oct-2011 - 16-Jul-2012

4. TITLE AND SUBTITLE
Cyclical dynamics and control of a neuromechanical system: Final Report

5a. CONTRACT NUMBER
W911NF-11-1-0495

5b. GRANT NUMBER

5c. PROGRAM ELEMENT NUMBER
611102

6. AUTHORS
Eric D. Tytell

5d. PROJECT NUMBER

5e. TASK NUMBER

5f. WORK UNIT NUMBER

7. PERFORMING ORGANIZATION NAMES AND ADDRESSES
Johns Hopkins University
Johns Hopkins University
3400 N. Charles St.
Baltimore, MD 21218 -2686

8. PERFORMING ORGANIZATION REPORT NUMBER

9. SPONSORING/MONITORING AGENCY NAME(S) AND ADDRESS(ES)
U.S. Army Research Office
P.O. Box 12211
Research Triangle Park, NC 27709-2211

10. SPONSOR/MONITOR'S ACRONYM(S)
ARO

11. SPONSOR/MONITOR'S REPORT NUMBER(S)
60787-EG-II.1

12. DISTRIBUTION AVAILIBILITY STATEMENT
Approved for Public Release; Distribution Unlimited

13. SUPPLEMENTARY NOTES
The views, opinions and/or findings contained in this report are those of the author(s) and should not contrued as an official Department of the Army position, policy or decision, unless so designated by other documentation.

14. ABSTRACT
In this project, we used computational models to analyze how the intrinsic dynamical properties of neural and mechanical systems interact to produce stable, but adaptable locomotion. Animal locomotion is a rhythmic behavior that requires the effective coupling of multiple feedback loops, including mechanical coupling between the animal's body and the environment, coupling between muscular force production and body movement, and sensory feedback. Floquet theory, a branch of nonlinear dynamics, includes ways to analyze how such rhythmic

15. SUBJECT TERMS
neural control, biomechanics, muscle, nonlinear dynamics, Floquet analysis

16. SECURITY CLASSIFICATION OF:			17. LIMITATION OF ABSTRACT	15. NUMBER OF PAGES	19a. NAME OF RESPONSIBLE PERSON
a. REPORT	b. ABSTRACT	c. THIS PAGE			Eric Tytell
UU	UU	UU	UU		19b. TELEPHONE NUMBER 617-627-3195

Report Title

Cyclical dynamics and control of a neuromechanical system: Final Report

ABSTRACT

In this project, we used computational models to analyze how the intrinsic dynamical properties of neural and mechanical systems interact to produce stable, but adaptable locomotion. Animal locomotion is a rhythmic behavior that requires the effective coupling of multiple feedback loops, including mechanical coupling between the animal's body and the environment, coupling between muscular force production and body movement, and sensory feedback. Floquet theory, a branch of nonlinear dynamics, includes ways to analyze how such rhythmic systems respond to perturbations. We developed several robust ways of estimating the Floquet modes of a rhythmic system, which are canonical patterns of activity after a perturbation. We found that when a block of muscle is forced to change length sinusoidally and is cyclically activated, it is strongly self-stabilizing, even with no sensory feedback. When two muscles act antagonistically, as they do around most vertebrate joints, then the system is less stable naturally. However, with sensory feedback, the joint can be stabilized very easily. This research may be extended to analyze Floquet modes based on empirical data, to examine the stability properties of real muscle, and to study the stability of fish swimming and control potential of fish fins.

Enter List of papers submitted or published that acknowledge ARO support from the start of the project to the date of this printing. List the papers, including journal references, in the following categories:

(a) Papers published in peer-reviewed journals (N/A for none)

Received Paper

TOTAL:

Number of Papers published in peer-reviewed journals:

(b) Papers published in non-peer-reviewed journals (N/A for none)

Received Paper

TOTAL:

Number of Papers published in non peer-reviewed journals:

(c) Presentations

Number of Presentations: 0.00

Non Peer-Reviewed Conference Proceeding publications (other than abstracts):

Received Paper

TOTAL:

Number of Non Peer-Reviewed Conference Proceeding publications (other than abstracts):

Peer-Reviewed Conference Proceeding publications (other than abstracts):

Received Paper

TOTAL:

Number of Peer-Reviewed Conference Proceeding publications (other than abstracts):

(d) Manuscripts

Received	Paper

TOTAL:

Number of Manuscripts:

Books

Received	Paper

TOTAL:

Patents Submitted

Patents Awarded

Awards

Graduate Students

NAME	PERCENT_SUPPORTED
FTE Equivalent:	
Total Number:	

Names of Post Doctorates

NAME	PERCENT_SUPPORTED
Sean Carver	0.30
FTE Equivalent:	**0.30**
Total Number:	**1**

Names of Faculty Supported

NAME	PERCENT_SUPPORTED	National Academy Member
Eric Tytell	0.44	
FTE Equivalent:	**0.44**	
Total Number:	**1**	

Names of Under Graduate students supported

NAME	PERCENT SUPPORTED

FTE Equivalent:

Total Number:

Student Metrics

This section only applies to graduating undergraduates supported by this agreement in this reporting period

The number of undergraduates funded by this agreement who graduated during this period:	0.00
The number of undergraduates funded by this agreement who graduated during this period with a degree in science, mathematics, engineering, or technology fields:.....	0.00
The number of undergraduates funded by your agreement who graduated during this period and will continue to pursue a graduate or Ph.D. degree in science, mathematics, engineering, or technology fields:.....	0.00
Number of graduating undergraduates who achieved a 3.5 GPA to 4.0 (4.0 max scale):	0.00
Number of graduating undergraduates funded by a DoD funded Center of Excellence grant for Education, Research and Engineering:	0.00
The number of undergraduates funded by your agreement who graduated during this period and intend to work for the Department of Defense	0.00
The number of undergraduates funded by your agreement who graduated during this period and will receive scholarships or fellowships for further studies in science, mathematics, engineering or technology fields:	0.00

Names of Personnel receiving masters degrees

NAME

Total Number:

Names of personnel receiving PHDs

NAME

Total Number:

Names of other research staff

NAME	PERCENT SUPPORTED

FTE Equivalent:

Total Number:

Sub Contractors (DD882)

Inventions (DD882)

Scientific Progress

See attached.

Technology Transfer

Cyclical dynamics and control of a neuromechanical system: Final Report

Eric D. Tytell
Department of Mechanical Engineering, Johns Hopkins University,
tytell@jhu.edu*

Abstract

In this project, we used computational models to analyze how the intrinsic dynamical properties of neural and mechanical systems interact to produce stable, but adaptable locomotion. Animal locomotion is a rhythmic behavior that requires the effective coupling of multiple feedback loops, including mechanical coupling between the animal's body and the environment, coupling between muscular force production and body movement, and sensory feedback. Floquet theory, a branch of nonlinear dynamics, includes ways to analyze how such rhythmic systems respond to perturbations. We developed several robust ways of estimating the Floquet modes of a rhythmic system, which are canonical patterns of activity after a perturbation. We found that when a block of muscle is forced to change length sinusoidally and is cyclically activated, it is strongly self-stabilizing, even with no sensory feedback. When two muscles act antagonistically, as they do around most vertebrate joints, then the system is less stable naturally. However, with sensory feedback, the joint can be stabilized very easily. This research may be extended to analyze Floquet modes based on empirical data, to examine the stability properties of real muscle, and to study the stability of fish swimming and control potential of fish fins.

Animals must move effectively through complex, unpredictable environments. As they move, neural circuits called central pattern generators (CPGs) produce a basic pattern of muscle activity (Grillner, 2003), activating muscles that move the body, which interacts with the external environment (Tytell et al., 2011). At the same time, the environment produces forces back on the body, influencing the motion (Jordan, 1996), and the CPG receives sensory inputs that modulate the locomotor pattern (Rossignol et al., 2006) (see Fig. 1). Each of these components has its own intrinsic dynamical properties, but all of them must work together to produce a stable pattern.

In this project, we investigated how neural and mechanical systems can work together to produce stable cyclical dynamics. Specifically, we examined how such systems respond to perturbations: small disturbances away from the normal pattern, called a *limit cycle*. For some perturbations, the system rapidly returns to its normal limit cycle; for other perturbations, the activity pattern changes for long periods of time.

*Current address: Department of Biology, Tufts University, eric.tytell@tufts.edu

A branch of dynamical systems theory called Floquet analysis (Floquet, 1883; Guckenheimer and Holmes, 1983) allows one to classify these types of perturbations. The state of the system $\mathbf{x}(t)$ can be defined in a high-dimensional state space ($\mathbb{R}^P$), where $\mathbf{x}$ might include all of the membrane potentials and synaptic conductances of neurons in the CPG model, or the lengths, velocities, and calcium concentrations in a muscle model. Since the system is periodic, $\mathbf{x}(t)$ traces out a closed loop γ in the $n-$dimensional space. A perturbation means that the system will deviate from the limit cycle:

$$\mathbf{z}(t) = \mathbf{x}(t) - \mathbf{x}^*(t), \tag{1}$$

where $\mathbf{x}^*(t)$ is on the limit cycle γ.

For a particular system, Floquet analysis allows one to define a set of canonical modes $\mathbf{u}_k(t)$ that are particular patterns of deviations from the limit cycle. The modes are the axes of a new coordinate system, centered on the limit cycle, that rotates and stretches about the cycle. Even though the modes may be complicated, when the state of the system is expressed in this new coordinate system, the dynamics become very simple: any perturbation simply decays exponentially back to the limit cycle. The rate of decay is quantified by the Floquet exponent μ_k, so that the deviation from the limit cycle can be written as

$$\mathbf{z}(t) = e^{\mu_k t}\mathbf{u}_k(t). \tag{2}$$

Negative Floquet exponents correspond to stable patterns, and the more negative the exponent, the more rapidly the perturbation dies away.

The goal of this project was to examine how the intrinsic dynamics of neural and mechanical systems interact in a computational model, based on the lamprey. The primary results of the work were

- Several robust techniques were developed for estimating limit cycles and Floquet modes. In particular, we developed a technique for finding Floquet modes that does not require any integration. These techniques may be used when the state equation is known, but also potentially on empirical data.
- We found that muscle is strongly self-stabilizing when activated cyclically, possibly because of the nonlinearity in how calcium binds and releases from muscle filaments. Two muscles in an

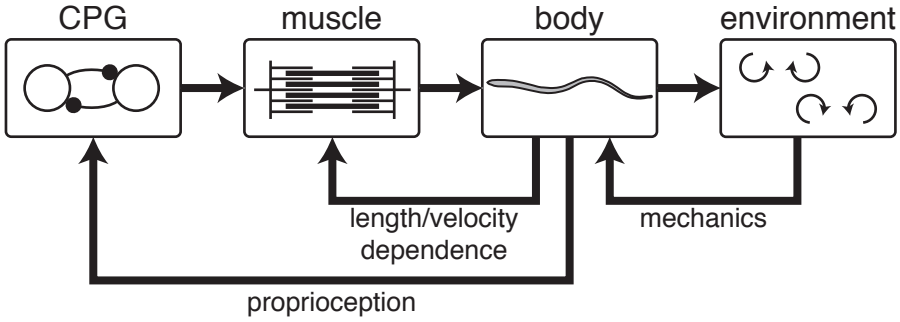

Figure 1: Diagram of the nested feedback loops that make up a neuromechanical system. A central pattern generator circuit activates muscle that produces force to bend the body, which interacts with the environment. At the same time, the environment produces reaction forces back on the body ("mechanics"), muscle force is coupled with body motion due to length and velocity dependence, and the CPG receives proprioceptive sensory inputs.

antagonistic arrangement, similar to that of most vertebrate joints, have a less stable mode that would need to be corrected by sensory feedback, but may also provide a simple way to control turning.
- Preliminary evidence was found for an optimal feedback strength for maximum stability in the neuromechanical system.

These findings suggest several avenues to continue and extend this work:

- The harmonic balance technique may be appropriate for extracting limit cycles and Floquet modes from data. Further work will be necessary to establish the feasibility and accuracy of this approach.
- The analysis of the muscle model makes some strong predictions about the stability of cyclically driven muscle. The model approximates a standard experimental configuration called a "work loop"; thus, these predictions may be possible to test experimentally.
- The ideas developed here may be applicable to understanding the stability and control of fish swimming. By using stimulating electrodes to introduce phase-locked perturbations to the muscles of a swimming fish, we may be able to rigorously evaluate the phase-dependent control potential of fish fins, and how fish use them to maintain stability.

Details of both the findings and the future directions follow.

1 Primary findings

1.1 Robust techniques for estimating limit cycles and Floquet modes

Much of the project period was spent developing numerical methods for robust estimation of limit cycles and Floquet modes. The numerical problem is made particularly difficult because we needed to detect relatively tiny deviations from the relatively large limit cycle.

1.1.1 Limit cycles

Shooting methods Initially, we proceeded based on the idea of a Poincaré section: a hyperplane of co-dimension $P-1$ that intersects the limit cycle transversely. The (linearized) return map, $\mathbf{J}$, (also called a Poincaré map) describes locally how perturbations from a point $\mathbf{x}^*(t)$ recover after one full cycle of the nonlinear dynamics. Given a system defined as

$$\dot{\mathbf{x}} = f(\mathbf{x}), \quad \mathbf{x} \in \mathbb{R}^P, \tag{3}$$

one can integrate the dynamics of a point $\mathbf{x}_0$ that starts on the hyperplane until it returns to the same plane at another point $\mathbf{x}_1$.

As a method for estimating the limit cycle, this forward integration, called a "shooting" technique, works well. One starts with a candidate point close to the limit cycle $\mathbf{x}_{fp,0}$ and integrates to find the first return $\mathbf{x}_{fp,1}$. Then, using a standard minimization technique such as Newton's method, one can minimize the difference $|\mathbf{x}_{fp,0} - \mathbf{x}_{fp,1}|$.

Harmonic balance technique One can also estimate the limit cycle as a Fourier series. This method is attractive because it implicitly enforces the limit cycle solution to be periodic. Full details are given in Appendix A. The approximation method is quite similar to that used by Bonani and Gilli (1999). For system (3), choose the coefficients of a Fourier series that produces a candidate cycle $\hat{\mathbf{x}}$. If $\hat{\mathbf{x}}$ were on the true limit cycle,

$$\dot{\hat{\mathbf{x}}} - f(\hat{\mathbf{x}}) = 0. \tag{4}$$

The derivative of a Fourier series can be easily expressed in terms of the coefficients of the original series, which allows one to simplify $\dot{\hat{\mathbf{x}}}$. Furthermore, (4) holds at each point along the limit cycle, which means one can discretize the problem into M equations, each at a different phase. Then the coefficients of the Fourier series can be found by standard multivariate minimization procedures, such as Matlab's `fsolve` function. See Appendix A for details. Interestingly, this procedure could also be used to find an *unstable* limit cycle.

1.1.2 Floquet modes

In principle, one can extend the shooting technique to estimate the linearized return map $\mathbf{J}(T)$. $\mathbf{J}(0) = \mathbf{I}^P$, the P-dimensional identity matrix. $\mathbf{J}(t)$ can be estimated by integrating

$$\dot{\mathbf{J}}(t) = \mathbf{A}(t)\mathbf{J}(t), \tag{5}$$

where $\mathbf{A}(t)$ is the derivative matrix

$$\mathbf{A}(t) = \left.\frac{\partial f}{\partial x_j}\right|_{\mathbf{x}\in\gamma} \tag{6}$$

evaluated on the limit cycle. Then $\mathbf{J}(T)$ is estimated by integrating (5) from 0 to T, where T is the period (Apri et al., 2010; Guckenheimer and Holmes, 1983). The eigenvalues and eigenvectors of $\mathbf{J}(T)$ correspond to the Floquet multipliers M_k (where $M_k = e^{\mu_k T}$) and the modes at time t.

However, this technique fails when the exponents are large and negative, or when they are close to zero but not exactly equal to zero (Fairgrieve and Jepson, 1991; Lust, 2001). When exponents are large and negative, perturbations die out extremely rapidly, and the Floquet modes are entirely swamped by numerical error in the integration over a full period. Similarly, it becomes very difficult to distinguish modes with exponents that are exactly zero from those that are close to but not equal to zero, for the same reason that small differences become swamped in numerical error over the integration period.

A better approach is to approximate the Floquet modes as Fourier series. This method is similar to the one developed by Traversa and Bonani in a series of papers characterizing the noise in oscillatory electrical circuits (Bonani and Gilli, 1999; Traversa and Bonani, 2011a,b; Traversa et al., 2008). With some careful approximation and discretization, **finding Floquet modes becomes a simple eigenvalue problem, requiring no integration**.

Linearizing (3) about the limit cycle and using (3), one obtains

$$\dot{\mathbf{z}} - \mathbf{A}(t)\mathbf{z} = 0. \tag{7}$$

If $\hat{\mathbf{u}}_k$ is a Fourier approximation of a candidate Floquet mode of the system, and $\hat{\mu_k}$ is the approximation of its Floquet exponent, then

$$\mathbf{z}(t) = e^{\hat{\mu}_k t}\hat{\mathbf{u}}_k(t) \tag{8}$$

should be a solution of (7). Substituting into (7), we find

$$\hat{\mu}_k \hat{\mathbf{u}}_k(t) + \dot{\hat{\mathbf{u}}}_k(t) - \mathbf{A}(t)\hat{\mathbf{u}}_k(t) = 0 \tag{9}$$

after factoring out $e^{\hat{\mu}_k t}$. Again, since we express $\hat{\mathbf{u}}_k(t)$ as a Fourier series, we can easily write the coefficients of $\dot{\hat{\mathbf{u}}}_k$ in terms of the original coefficients. We discretize at M phase values along the limit cycle. In the end, the modes and their exponents end up as eigenvectors and eigenvalues of a large matrix that is primarily constructed from the values of the derivative matrix $\mathbf{A}$ evaluated at the M phases. See Appendix B for details.

1.2 Intrinsic stability of muscle

Previous work has suggested that muscle can be self-stabilizing for static force production (e.g. McMahon, 1984), but no one has investigated this idea in the context of cyclical motions, which are much more common. In addition, most of the previous work has examined muscle together with its sensory feedback (e.g. Prochazka et al., 1997). We found that **muscle, with only its natural calcium dynamics and length, velocity, and tension relationships, is strongly self-stabilizing**. I plan to submit these results as an abstract to present at the Society for Integrative and Comparative Biology annual meeting in January, 2013, and I anticipate writing up and publishing them in the near future.

Brief description of the muscle model The model of muscle is taken from Williams et al. (1998), who developed it for lamprey muscle, but the structure of the model is appropriate for many different vertebrate muscles. Briefly, muscle consists of a contractile element and a series elastic element (Fig. 2). The contractile element produces force P_c that depends on its length l_c, contraction velocity v_c, and the amount Caf of calcium that is bound to the contractile filaments:

$$P_c = P_0 \lambda(l_c)\xi(v_c)Caf, \tag{10}$$

where P_0 is the maximum force. The functions $\lambda(l_c)$ and $\xi(v_c)$ define the length-tension and velocity-tension relationships:

$$\lambda(l_c) = 1 + \lambda_2(l_c - l_{c0}) \tag{11}$$

$$\xi(v_c) = 1 + \begin{cases} \xi_m v_c, & \text{if } v_c \le 0, \\ \xi_p v_c, & \text{if } v_c > 0. \end{cases} \tag{12}$$

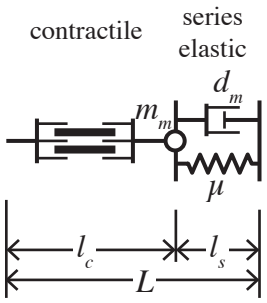

Figure 2: Diagram of the muscle model, showing the contractile element on the left and the series elastic element and damper on the right.

The calcium dynamics can be written with two states:

$$\dot{Ca} = (k_4 Caf - k_3 Ca)(1 - Caf) + Ca_{act}, \tag{13}$$

$$\dot{Caf} = -(k_4 Caf - k_3 Ca)(1 - Caf), \tag{14}$$

where Ca_{act} depends on the neural activation g_{act}, which is scaled to be between 0 and 1:

$$Ca_{act} = k_1 g_{act}(C - Ca - Caf) + k_2(1 - g_{act})Ca(C - S - Ca - Caf). \tag{15}$$

Finally, the whole muscle element is a spring-mass-damper system:

$$m_m \ddot{l_c} + d_m \dot{l_c} - \mu(L - l_c - l_{s0}) = P_c, \tag{16}$$

where M is the mass of the muscle element (called a sarcomere), D is the damping, μ is the stiffness of the series elastic element, L is the total sarcomere length, and l_{s0} is the resting length of the series elastic element (Fig. 2).

Stability of a cyclically driven muscle segment Based on this model, one can examine a cyclical system in which the muscle length is forced to change sinusoidally ($L = A\sin(2\pi ft)$) and the muscle is activated at a particular phase ϕ_{act} during the cycle. This is the so-called "work loop" method used in numerous experimental studies (e.g. Josephson and Stokes, 1999).

For ease of comprehension, we use a "half-life" as a way to compare the Floquet exponents. This is the time that it takes for half of the perturbation to die out: $t_{1/2} = \log(0.5)/\mu_k$, where μ_k is the Floquet exponent.

In the work loop configuration, the slowest Floquet mode has a half life of 10.1% of a cycle, regardless of the phase of activation. (Note that unlike autonomous systems, this is a driven system, so there is no mode with an exponent of zero.) All others modes die away much more quickly, in 2% or less of a cycle. Because of the short time constant of the mode, perturbations have a small effect in general. Fig. 3a shows the effect on force production of a 20% perturbation along the first Floquet mode. Note that all effects are small and die away rapidly, even though the perturbation is very large compared to physiological changes, which tend to be around $\pm 5\%$. Similarly, the effect on total work done is small, regardless of the phase of activity or the phase of the perturbation (Fig. 3b). This stability seems to be related to the calcium dynamics, because changing the calcium rate constants can increase the duration of the first Floquet mode. Increasing k_4 (the rate that calcium is released from the filaments) or decreasing k_3 (the rate that calcium binds to the filaments) tend to increase the stability of the muscle; either change results in less calcium bound to the filaments.

Stability of two antagonistic muscles The work-loop configuration is simple and is interesting because of the large literature, but it is not a very realistic situation. A more realistic model would be two antagonistic muscles, pulling on a mass-spring-damper system, similar to the muscles that move a fish's tail from side to side, or to the extensor and flexor muscles that move a leg forward and back. Here, the two muscles are activated in anti-phase at a frequency f_{act}. At the same time, the mass-spring-damper has a mechanical resonant frequency f_{res} and a damping coefficient ζ. **This configuration shows evidence for the necessity of sensory feedback, but, at the same time, the possibility of using natural dynamics to steer an organism.**

In this configuration, a new, slower mode appears, with a half life of as much as 80% of a cycle (Fig. 4a). The time constant of the mode depends on the mechanical resonant frequency and the damping coefficient. The second mode (Fig. 4b) is the same as the first mode with a single muscle, seen above, and does not depend on frequency. The first mode exclusively affects the position and velocity of the mass (Fig. 4c), and the corresponding lengths of the muscle segments. In other words, because two identical muscles pulling against each other produce forces that are very nearly matched, if the mass is perturbed off its center position, then it takes a long time to return to the center position.

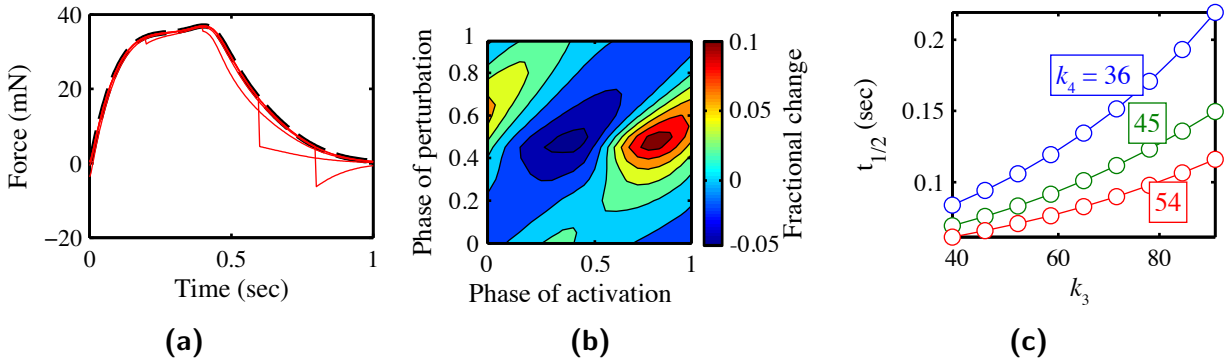

Figure 3: Perturbations have a relatively small effect on a single, cyclically driven muscle. (a) Change in force due to 20% perturbations along the slowest Floquet mode. Black dashed line shows steady-state force production; red lines show perturbations. (b) Contour plot showing the change in total work done after a 20% perturbation along the slowest Floquet mode, relative to the phase of activation and the phase of the perturbation. Note that all changes are less than about $\pm 10\%$. (c) Half life of the slowest Floquet mode as a function of calcium parameters. The stability of muscle seems to depend primarily on the calcium dynamics.

This slow mode points to a **situation where neural and mechanical systems must work together, each compensating for the other**. In this case, a CPG driving the two antagonistic muscles would only need to monitor and correct the mean position of the mass, in order to cancel out the slow mode and produce extremely stable cyclical motion. Alternatively, to produce turning, the nervous system would only need to generate a brief perturbation in the position of the mass to cause a long lasting deviation to one side, which would cause a turn for a swimming organism.

1.3 Role of feedback

We are currently working to simulate and understand the full neuromechanical model shown in Fig. 1. Preliminary results suggest that the system is also quite stable, but that there is an optimal feedback strength for maximal stability (Fig. 5). These simulations are computationally intensive to perform in Matlab, and may require some optimization in order to be tractable.

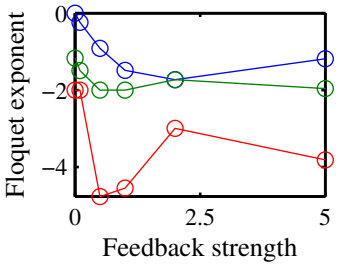

Figure 5: Preliminary results showing the first three non-zero Floquet exponents for the complete neuromechanical system, shown in Fig. 1, as the strength of the proprioceptive feedback varies. Note that there seems to be a minimum value for the exponent shown in blue at a feedback strength of 2.

2 Future directions

This project has generated many useful ideas that should be elaborated and studied further.

2.1 Estimation of limit cycles and Floquet modes from data

A goal of this project was to develop numerical analysis techniques that might be appropriate for use on data, not just on sim-

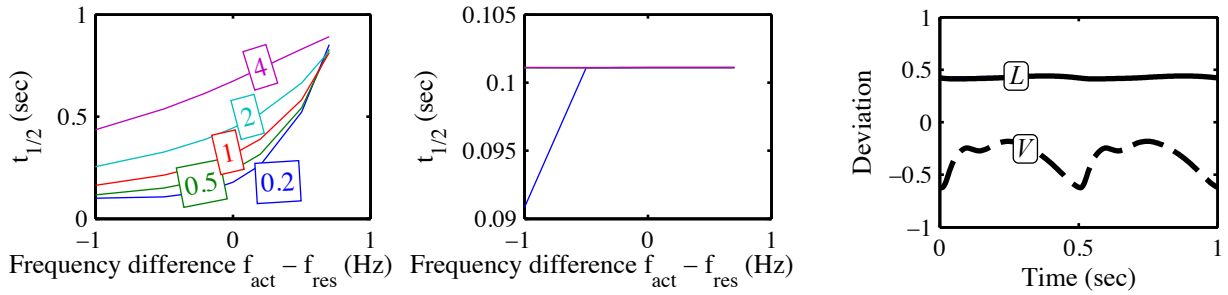

(a) Mode 1 **(b)** Mode 2 **(c)** Effect of mode 1

Figure 4: With two antagonistic muscles, a slower mode appears that depends on the resonance and damping of the mass on which the muscles pull. **(a)** Half-life of mode 1 as a function of the difference of the activation frequency f_{act} and the mechanical resonant frequency f_{res}, and as a function of the damping coefficient ζ. **(b)** Half-life of mode 2 for the same cases as in panel (a). **(c)** Effect of mode 1 on the position L and velocity V of the mass for $f_{act} - f_{res} = 0.7$ and $\zeta = 4$.

ulations. The harmonic balance technique developed here may be adapted for estimating limit cycles from data, and may even be used for estimating Floquet modes. I briefly describe how this might be possible; further work will be necessary to establish the feasibility of this approach. As I elaborate these ideas further, I plan to develop a manuscript for publication.

Estimating limit cycles To estimate a limit cycle from data, one can perform essentially the same optimization approach described in Appendix A. Given a noisy time series data set $\mathbf{X}(t_i)$ at many times t_i, one can estimate $\dot{\mathbf{x}}$ numerically by central differences as $d\mathbf{X}$. Again, choose a Fourier approximation for a candidate limit cycle $\hat{\mathbf{x}}$. Interpolate the estimated state velocity $d\mathbf{X}$ on to the candidate limit cycle. Then, optimize the limit cycle to minimize

$$\dot{\hat{\mathbf{x}}} - d\mathbf{X}|_{\mathbf{x}=\hat{\mathbf{x}}} \,. \tag{17}$$

As before $\dot{\hat{\mathbf{x}}}$ can be expressed in terms of the original Fourier coefficients. One would have to impose some smoothness constraint on $\hat{\mathbf{x}}$; otherwise, it might wiggle around to every data point. Also, one might need to have some outlier detection for velocities. Some values of $d\mathbf{X}$ might represent the true state velocity of the system, but others will be noise.

Estimating Floquet modes To use the harmonic balance approach to estimate Floquet modes, one only needs to know the limit cycle (which may be estimated using the technique above) and the value of the derivative matrix *on the limit cycle*. The derivative matrix does not need to be evaluated everywhere. Estimating a high-dimensional derivative matrix is challenging, but it will be significantly easier to estimate on a small number of points, rather than across the entire state space. To estimate the derivative matrix, it is probably best to introduce controlled perturbations, rather than trying to analyze existing time series. These ideas inform some of the experiments proposed in §2.3.

2.2 Stability properties of muscle

The observations described above (§1.2) make strong predictions about the behavior of muscle. Such predictions can be tested, at least to some extent, using *in vitro* muscle physiological experiments. The work loop technique used as a baseline model of muscle is an experimental technique (e.g. Josephson, 1993). Thus, one could perform physical experiments that are quite similar to the computational models developed here, in order to test the predictions of the model.

An experimental challenge, however, is measuring and perturbing the system's state. Total length and velocity are straightforward to measure and manipulate, but one cannot measure the state of the contractile element separately. However, one can measure the elasticity of the series elastic element, and to some extent the passive damping properties of the muscle (McMahon, 1984), which would enable an estimate of the state of the contractile element. Calcium concentrations are possible to measure using calcium sensitive fluorescent dyes (Vergara et al., 1991), but can only be perturbed over long time periods by changing total calcium concentrations in the saline bath holding the muscle fiber.

Such experiments, while challenging, may help to establish further the self-stabilizing properties of muscle during cyclical motions.

2.3 Control potential of fish fins

Inspired by these computational results and the experiments of Sponberg et al. (2011a,b), I am developing experiments to examine the stability of fish as they are swimming and establish the control potential of fish fins. In these experiments, we will implant fine wire electromyographic electrodes (e.g. Tytell and Lauder, 2002) in both the axial red muscles that power the side-to-side motions of the body and tail, and in the smaller muscles that control the motions of the dorsal and anal fins. These electrodes will serve a dual purpose: they will both record muscle activity and will also be able to stimulate the muscle to contract. My previous work has shown that the dorsal and anal fins are not passive keels, but actively generate substantial forces (Tytell, 2006).

Using the techniques described above (§2.1), we will estimate the steady limit cycle, including both three-dimensional kinematic data and muscle activity. Then, we will perturb the muscle activity, stimulating the muscles at particular phases in the swimming cycle. This will allow us to measure the control potential of the fins as a function of phase, and to estimate something analogous to Floquet modes. Because we cannot measure all of the states of the swimming fish, we will only be able to estimate these modes in a smaller subspace.

Nevertheless, controlled perturbations of this sort will be informative and perhaps surprising. Sponberg et al. (2011b) found that a muscle in the cockroach leg produced a very different effect when it was stimulated during the running cycle, compared to its effect during standing. Similarly, we might expect counterintuitive results from out experiments. For example, fins have muscles called "elevators" that elevate the fin rays, making the fin area larger. If the fish is stationary, these muscles probably have very little effect on forward propulsion. During swimming, however, they may have a large effect, because they change the fin area.

Appendices

A Harmonic balance approach for estimating limit cycles

The approach described below is quite similar to that developed in papers by Traversa and Bonani (Bonani and Gilli, 1999; Traversa and Bonani, 2011a; Traversa et al., 2008).

Consider a dynamical system defined as

$$\dot{\mathbf{x}} - f(\mathbf{x}) = 0, \tag{18}$$

where $\mathbf{x}$ is a state variable in P dimensions. We are aiming to write the dynamical system as a set of equations for the Fourier components of the solution.

Write the limit cycle solution $\mathbf{x}(t)$ in terms of N harmonic components for each of the i dimensions:

$$x_i(t) = x^f_{i0} + \sum_{k=1}^{N} \left[x^f_{cik} \cos(k\omega t) + x^f_{sik} \sin(k\omega t) \right]. \tag{19}$$

Based on the coefficients, define a $P(2N+1)$ component frequency state vector

$$\mathbf{x}^f = \begin{bmatrix} x^f_{10} & x^f_{c11} & x^f_{s11} & \cdots & x^f_{c1N} & x^f_{s1N} & x^f_{20} & x^f_{c21} & x^f_{s21} & \cdots & x^f_{cPN} & x^f_{sPN} \end{bmatrix}^T \tag{20}$$

that consists of the components for each dimension stacked on top of each other.

Now let's sample the system at M samples in time, spread evenly through the period $T = 2\pi/\omega$:

$$t_j = \frac{2\pi}{\omega} \frac{j}{M} \tag{21}$$

where $M \geq 2N+1$. Define a time-sampled state vector, similar to the frequency state vector

$$\mathbf{x}^t = \begin{bmatrix} x_1(t_1) & x_1(t_2) & \cdots & x_1(t_M) & x_2(t_1) & x_2(t_2) & \cdots & x_P(t_M) \end{bmatrix}^T \tag{22}$$

Then we can write $\mathbf{x}^t$ and $\mathbf{x}^f$ in terms of each other by multiplying by a constant matrix Γ^{-1}:

$$\mathbf{x}^t = \Gamma^{-1}\mathbf{x}^f \qquad \mathbf{x}^f = \Gamma\mathbf{x}^t. \tag{23}$$

The matrix Γ^{-1} consists of an $M \times 2N+1$ dimensional matrix Γ_0^{-1} that is repeated P times along the diagonal.

$$\Gamma_0^{-1} = \begin{bmatrix} 1 & \gamma_{c11} & \gamma_{s11} & \gamma_{c12} & \gamma_{s12} & \cdots & \gamma_{c1N} & \gamma_{s1N} \\ 1 & \gamma_{c21} & \gamma_{s21} & \gamma_{c22} & \gamma_{s22} & \cdots & \gamma_{c2N} & \gamma_{s2N} \\ \vdots & & & & & \ddots & & \vdots \\ 1 & \gamma_{cM1} & \gamma_{sM1} & \gamma_{cM2} & \gamma_{sM2} & \cdots & \gamma_{cMN} & \gamma_{sMN} \end{bmatrix} \tag{24}$$

where

$$\gamma_{cjk} = \cos(2\pi jk/M) \tag{25}$$

$$\gamma_{sjk} = \sin(2\pi jk/M), \tag{26}$$

and finally

$$\Gamma^{-1} = \begin{bmatrix} \Gamma_0^{-1} & 0 & \cdots & 0 \\ 0 & \Gamma_0^{-1} & \cdots & 0 \\ \vdots & & \ddots & \vdots \\ 0 & 0 & \cdots & \Gamma_0^{-1} \end{bmatrix} \tag{27}$$

with P repetitions of Γ_0^{-1}.

We can express $\dot{\mathbf{x}}$ easily

$$\dot{x}_i(t) = \sum_{k=1}^{N} -x_{cik}^f k\omega \sin(k\omega t) + x_{sik}^f k\omega \cos(k\omega t) \tag{28}$$

or

$$\dot{\mathbf{x}}^f = \omega \Omega \mathbf{x}^f, \tag{29}$$

where Ω is a constant matrix. Again, we have an $M \times 2N+1$ dimensional matrix Ω_0

$$\Omega_0 = \begin{bmatrix} 0 & 0 & 0 & 0 & 0 & \cdots & 0 & 0 \\ 0 & 0 & 1 & 0 & 0 & \cdots & 0 & 0 \\ 0 & -1 & 0 & 0 & 0 & \cdots & 0 & 0 \\ 0 & 0 & 0 & 0 & 2 & \cdots & 0 & 0 \\ 0 & 0 & 0 & -2 & 0 & \cdots & 0 & 0 \\ \vdots & & & & & \ddots & & \vdots \\ 0 & 0 & 0 & 0 & 0 & \cdots & 0 & N \\ 0 & 0 & 0 & 0 & 0 & \cdots & -N & 0 \end{bmatrix}. \tag{30}$$

where Ω is constructed by stacking Ω_0 P times along the diagonal.

Thus we have $2N+1$ equations for the $2N+1$ coefficients and the frequency ω. We need an additional condition to solve for the frequency. Following Bonani and Gilli (1999), we set $x_{s11}^f = 0$, which amounts to saying that the initial phase of the oscillator is arbitrary.

We can solve for the $2N+1$ coefficients and the frequency ω with the following set of at least $2N+2$ equations

$$Q(\mathbf{x}^f, \omega) = \begin{cases} \omega \Omega \mathbf{x}^f - \Gamma f(\Gamma^{-1}\mathbf{x}^f) & = 0 \\ x_{s11}^f & = 0 \end{cases} \tag{31}$$

The last condition amounts to saying that the phase of the oscillator is arbitrary Bonani and Gilli (1999).

For rapid numerical solution, we can also write the Jacobian of the system $Q(\mathbf{x}^f, \omega)$ from Eqs. (31),

$$\frac{\partial Q}{\partial \begin{bmatrix} \mathbf{x}^f & \omega \end{bmatrix}} = \begin{bmatrix} \omega\Omega - \Gamma Df \Gamma^{-1} & \Omega \mathbf{x}^f \\ \begin{bmatrix} 0 & 0 & 1 & 0 & \cdots & 0 \end{bmatrix} & 0 \end{bmatrix} \tag{32}$$

where Df is an $MP \times MP$ matrix with the following elements arrayed along the diagonal

$$\begin{bmatrix} \frac{\partial f}{\partial x_1}(t_1) & \frac{\partial f}{\partial x_1}(t_2) & \cdots & \frac{\partial f}{\partial x_1}(t_M) & \frac{\partial f}{\partial x_2}(t_1) & \cdots & \frac{\partial f}{\partial x_P}(t_M) \end{bmatrix} \tag{33}$$

The system converges pretty well using Matlab's `fsolve` function, except that there are multiple zeros when $\omega = (2\pi k)/T$, where T is the fundamental period and $k > 1$. It's easy to check, though, because the higher harmonics should be lower in magnitude than the first harmonics, by definition, if ω represents the fundamental period:

$$x^f_{cik} < x^f_{ci1} \quad \text{and} \quad x^f_{sik} < x^f_{si1} \tag{34}$$

for all $k > 1$.

B Harmonic balance technique for estimating Floquet modes and multipliers

Having set up this whole big framework, it becomes trivial to estimate both the Floquet modes and multipliers. First, we consider the system from Eq. (18) and linearize around the limit cycle, so that $\mathbf{z}(t) = \mathbf{x}(t) - \mathbf{x}^*(t)$, where $\mathbf{x}^*(t)$ is the limit cycle. Then

$$\dot{\mathbf{z}} - \mathbf{A}(t)\mathbf{z} = 0, \tag{35}$$

where $\mathbf{A}(t)$ is the Jacobian of the state equation defined on the limit cycle,

$$\mathbf{A}(t) = \left.\frac{\partial f}{\partial \mathbf{x}}\right|_{\mathbf{x}^*(t)}. \tag{36}$$

If $\mathbf{u}_k(t)$ is a Floquet mode of the system, then

$$\mathbf{z}(t) = e^{\mu_k t}\mathbf{u}_k(t) \tag{37}$$

is a solution of Eq. (35) with initial condition $\mathbf{z}(0) = \mathbf{u}_k(0)$. Substituting in to Eq. (35), we find that

$$\mu_k \mathbf{u}_k(t) + \dot{\mathbf{u}}_k(t) - A(t)\mathbf{u}_k(t) = 0. \tag{38}$$

Then we again discretize at M time intervals to write $\mathbf{u}^t_k$, a time-sampled version of $\mathbf{u}_k(t)$, and the corresponding frequency components $\mathbf{u}^f_k$,

$$\mathbf{u}^t_k = \begin{bmatrix} u_{k1}(t_1) & u_{k1}(t_2) & \cdots & u_{k1}(t_M) & u_{k2}t_1 & \cdots & u_{kP}(t_M) \end{bmatrix}^T \tag{39}$$

$$\mathbf{u}^f_k = \begin{bmatrix} u^f_{k10} & u^f_{kc11} & u^f_{ks11} & \cdots & u^f_{kc1N} & u^f_{ks1N} & u^f_{20} & u^f_{kc21} & u^f_{ks21} & \cdots & u^f_{kcPN} & u^f_{ksPN} \end{bmatrix} \tag{40}$$

These are related by the same Γ matrix as before:

$$\mathbf{u}^t_k = \Gamma^{-1}\mathbf{u}^f_k \quad \text{and} \quad \mathbf{u}^f_k = \Gamma\mathbf{u}^t_k \tag{41}$$

We need to write a version of the $\mathbf{A}$ matrix sampled at M time points. If $A_{ij}(t)$ is the i, j component of $\mathbf{A}$ at time t, then we write $\mathbf{A}^t_{ij} = \operatorname{diag}\begin{bmatrix} A_{ij}(t_1) & A_{ij}(t_2) & \cdots & A_{ij}(t_M) \end{bmatrix}$, again taking each time-sampled value and aligning them on the diagonal. The entire time sampled $MP \times MP$ matrix $\mathbf{A}^t$ consists of the diagonal blocks

$$\begin{bmatrix} \mathbf{A}^t_{11} & \mathbf{A}^t_{12} & \cdot & \mathbf{A}^t_{1P} \\ \mathbf{A}^t_{21} & \mathbf{A}^t_{22} & \cdot & \mathbf{A}^t_{2P} \\ \vdots & & \ddots & \vdots \\ \mathbf{A}^t_{P1} & \mathbf{A}^t_{P2} & \cdot & \mathbf{A}^t_{PP} \end{bmatrix} \tag{42}$$

Having done that, we can write Eq. (38) in the frequency domain

$$\begin{aligned} 0 &= \Gamma\left[\mu_k \mathbf{u}_k^t + \dot{\mathbf{u}}_k^t - \mathbf{A}^t \mathbf{u}_k^t\right] && (43)\\ &= \mu_k \mathbf{u}_k^f + \omega\Omega \mathbf{u}_k^f - \Gamma\mathbf{A}^t\Gamma^{-1}\Gamma\mathbf{u}_k^t && (44)\\ &= \mu_k \mathbf{u}_k^f + \omega\Omega \mathbf{u}_k^f - \hat{\mathbf{A}}\mathbf{u}_k^f && (45) \end{aligned}$$

where $\hat{\mathbf{A}} = \Gamma\mathbf{A}^t\Gamma^{-1}$. Solving for the Floquet modes and multiplier is now just an eigenvalue problem:

$$\left(\omega\Omega - \hat{\mathbf{A}}\right)\mathbf{u}_k^f = -\mu_k \mathbf{u}_k^f. \tag{46}$$

There are $(2N+1)P$ eigenvalues μ_k^f of Eq. (46), which are arrayed in columns along the imaginary axis and are related to the P Floquet multipliers μ_k of Eq. (35) by the following

$$\mu_k^f = \mu_k + qi\omega \tag{47}$$

where $q = \pm 1 \ldots N$.

References

Apri, M., Molenaar, J. and De Gee, M. (2010). Efficient estimation of the robustness region of biological models with oscillatory behavior. PLoS ONE *5*, e9865.

Bonani, F. and Gilli, M. (1999). Analysis of stability and bifurcations of limit cycles in Chua's circuit through the harmonic-balance approach. IEEE Trans. Circuits Syst. I *46*, 881–890.

Fairgrieve, T. and Jepson, A. (1991). O.K. Floquet Multipliers. SIAM J. Numer. Anal. *28*, 1446–1462.

Floquet, G. (1883). Sur les équations différentielles linéaires à coefficients périodiques. Ann. École Norm. Sup. *12*, 47–88.

Grillner, S. (2003). The motor infrastructure: From ion channels to neuronal networks. Nature Rev. Neurosci. *4*, 573–586.

Guckenheimer, J. and Holmes, P. (1983). Nonlinear oscillations, dynamical systems, and bifurcations of vector fields. Springer-Verlag, New York.

Jordan, C. E. (1996). Coupling internal and external mechanics to predict swimming behavior: A general approach? Amer. Zool. *36*, 710–722.

Josephson, R. and Stokes, D. (1999). Work-dependent deactivation of a crustacean muscle. J. Exp. Biol. *202*, 2551–2565.

Josephson, R. K. (1993). Contraction Dynamics and Power Output of Skeletal Muscle. Annu. Rev. Physiol. *55*, 527–546.

Lust, K. (2001). Improved numerical Floquet multipliers. International journal of bifurcation and chaos in applied sciences and engineering *11*, 2389–2410.

McMahon, T. A. (1984). Muscles, Reflexes, and Locomotion. Princeton University Press, Princeton.

Prochazka, A., Gillard, D. and Bennett, D. J. (1997). Positive force feedback control of muscles. J. Neurophysiol. *77*, 3226–3236.

Rossignol, S., Dubuc, R. J. and Gossard, J. P. (2006). Dynamic sensorimotor interactions in locomotion. Physiol. Rev. *86*, 89–154.

Sponberg, S., Libby, T., Mullens, C. H. and Full, R. J. (2011a). Shifts in a single muscle's control potential of body dynamics are determined by mechanical feedback. Phil. Trans. Roy. Soc. Lond. B *366*, 1606–1620.

Sponberg, S., Spence, A. J., Mullens, C. H. and Full, R. J. (2011b). A single muscle's multifunctional control potential of body dynamics for postural control and running. Philosophical Transactions of the Royal Society B: Biological Sciences *366*, 1592–1605.

Traversa, F. L. and Bonani, F. (2011a). Frequency-domain evaluation of the adjoint Floquet eigenvectors for oscillator noise characterisation. IET Circuits Devices Syst. *5*, 46.

Traversa, F. L. and Bonani, F. (2011b). Asymptotic Stochastic Characterization of Phase and Amplitude Noise in Free-Running Oscillators. Fluct Noise Lett *10*, 207–221.

Traversa, F. L., Bonani, F. and Guerrieri, S. D. (2008). A frequency-domain approach to the analysis of stability and bifurcations in nonlinear systems described by differential-algebraic equations. Int. J. Circ. Theor. Appl. *36*, 421–439.

Tytell, E. D. (2006). Median fin function in bluegill sunfish, *Lepomis macrochirus*: Streamwise vortex structure during steady swimming. J. Exp. Biol. *209*, 1516–1534.

Tytell, E. D., Holmes, P. J. and Cohen, A. H. (2011). Spikes alone do not behavior make: Why neuroscience needs biomechanics. Curr. Opin. Neurobiol. *21*, 816–822.

Tytell, E. D. and Lauder, G. V. (2002). The C-start escape response of *Polypterus senegalus*: Bilateral muscle activity and variation during stage 1 and 2. J. Exp. Biol. *205*, 2591–2603.

Vergara, J., DiFranco, M., Compagnon, D. and Suarez-Isla, B. A. (1991). Imaging of calcium transients in skeletal muscle fibers. Biophysical Journal *59*, 12–24.

Williams, T. L., Bowtell, G. and Curtin, N. A. (1998). Predicting force generation by lamprey muscle during applied sinusoidal movement using a simple dynamic model. J. Exp. Biol. *201*, 869–875.